Inorg. Chem. **2007**, *46*, 2979–2987

Trinuclear Silver(I) Complexes of Fluorinated Pyrazolates

H. V. Rasika Dias,* Chammi S. Palehepitiya Gamage, Jeremy Keltner, Himashinie V. K. Diyabalanage, Ivan Omari, Yvonne Eyobo, Nadeeka R. Dias, Nathan Roehr, Lesly McKinney, and Theresa Poth

Department of Chemistry and Biochemistry, The University of Texas at Arlington, Arlington, Texas 76019

Received December 12, 2006

Silver pyrazolates $\{[3\text{-}(CF_3)Pz]Ag\}_3$, $\{[3\text{-}(CF_3),5\text{-}(CH_3)Pz]Ag\}_3$, $\{[3\text{-}(CF_3),5\text{-}(Ph)Pz]Ag\}_3$, $\{[3\text{-}(CF_3),5\text{-}(Bu^t)Pz]Ag\}_3$, and $\{[3\text{-}(C_3F_7),5\text{-}(Bu^t)Pz]Ag\}_3$ have been synthesized by treatment of the corresponding pyrazole with a slight molar excess of silver(I) oxide. This economical and convenient route gives silver pyrazolates in high (>80%) yields. X-ray crystal structures of $\{[3\text{-}(CF_3),5\text{-}(CH_3)Pz]Ag\}_3$, $\{[3\text{-}(CF_3),5\text{-}(Bu^t)Pz]Ag\}_3$, and $\{[3\text{-}(C_3F_7),5\text{-}(Bu^t)Pz]Ag\}_3$ show that these molecules have trinuclear structures with essentially planar to highly distorted Ag_3N_6 metallacycles. $\{[3\text{-}(CF_3),5\text{-}(CH_3)Pz]Ag\}_3$ forms extended columns via intertrimer argentophilic contacts (the closest Ag···Ag separation between the neighboring trimers are 3.355 and 3.426 Å). The trinuclear $\{[3\text{-}(CF_3),5\text{-}(Bu^t)Pz]Ag\}_3$ units crystallize in pairs, basically forming "dimers of trimers", with the six silver atom core of the adjacent trimers adopting a chair conformation. However, in these dimers of trimers, even the shortest intertrimer Ag···Ag distance (3.480 Å) is slightly longer than the van der Waals contact of silver (3.44 Å). $\{[3\text{-}(C_3F_7),5\text{-}(Bu^t)Pz]Ag\}_3$, which has two bulky groups on each pyrazolyl ring, shows no close intertrimer Ag···Ag contacts (closest intertrimer Ag···Ag distance = 5.376 Å). The Ag–N bond distances and the intratrimer Ag···Ag separations of the silver pyrazolates do not show much variation. However, their N–Ag–N angles are sensitive to the nature (especially, the size) of substituents on the pyrazolyl rings. The π-acidic $\{[3,5\text{-}(CF_3)_2Pz]Ag\}_3$ and $\{[3\text{-}(C_3F_7),5\text{-}(Bu^t)Pz]Ag\}_3$ form adducts with the π-base toluene. X-ray data show that they adopt extended columnar structures of the type $\{\mathbf{[Ag_3]_2}\cdot[\text{toluene}]\}_\infty$ and $\{\mathbf{[Ag_3]'}\cdot[\text{toluene}]\}_\infty$ ($\{[3,5\text{-}(CF_3)_2Pz]Ag\}_3 = \mathbf{[Ag_3]}$,$\{[3\text{-}(C_3F_7),5\text{-}(Bu^t)Pz]Ag\}_3 = \mathbf{[Ag_3]'}$), in which toluene interleaves and makes face-to-face contacts with $\{[3\text{-}(C_3F_7),5\text{-}(Bu^t)Pz]Ag\}_3$ or dimers of $\{[3,5\text{-}(CF_3)_2\text{-}Pz]Ag\}_3$.

Introduction

Trinuclear pyrazolate complexes of monovalent coinage metals (i.e., Cu(I), Ag(I), and Au(I)) represent an important class of compounds with interesting structures and fascinating properties.[1−39] They feature planar or distorted nine-membered M_3N_6 metallacycles and often show various types and degrees of intertrimer M···M contacts leading to supramolecular assemblies with chair, prismatic, and star-shaped dimers of trimers or chain structures.[21,23,38,39] Apart from the interests related to structural diversity, some of these coinage metal pyrazolates have been used for the examination of metallophilic interactions between closed-shell d^{10} metal

* To whom correspondence should be addressed. E-mail: dias@uta.edu. Phone: 817-272-3813.

(1) La Monica, G.; Ardizzoia, G. A. *Prog. Inorg. Chem.* **1997**, *46*, 151−238.
(2) Banditelli, G.; Bandini, A. L.; Bonati, F.; Goel, R. G.; Minghetti, G. *Gazz. Chim. Ital.* **1982**, *112*, 539−42.
(3) Raptis, R. G.; Fackler, J. P., Jr. *Inorg. Chem.* **1988**, *27*, 4179−82.
(4) Bonati, F.; Burini, A.; Pietroni, B. R.; Galassi, R. *Gazz. Chim. Ital.* **1993**, *123*, 691−5.
(5) Bonati, F.; Minghetti, G.; Banditelli, G. *Chem. Comm.* **1974**, 88−9.
(6) Barbera, J.; Elduque, A.; Gimenez, R.; Oro, L. A.; Serrano, J. L. *Angew. Chem., Int. Ed. Engl.* **1997**, *35*, 2832−5.
(7) Barbera, J.; Elduque, A.; Gimenez, R.; Lahoz, F. J.; Lopez, J. A.; Oro, L. A.; Serrano, J. L. *Inorg. Chem.* **1998**, *37*, 2960−7.
(8) Bovio, B.; Bonati, F.; Banditelli, G. *Inorg. Chim. Acta* **1984**, *87*, 25−33.
(9) Murray, H. H.; Raptis, R. G.; Fackler, J. P., Jr. *Inorg. Chem.* **1988**, *27*, 26−33.
(10) Singh, K.; Long, J. R.; Stavropoulos, P. *J. Am. Chem. Soc.* **1997**, *119*, 2942−3.
(11) Ardizzoia, G. A.; La Monica, G.; Maspero, A.; Moret, M.; Masciocchi, N. *Inorg. Chem.* **1997**, *36*, 2321−8.
(12) Ardizzoia, G. A.; Monica, G. L. *Inorg. Synth.* **1997**, *31*, 299−302.
(13) Kim, S. J.; Kang, S. H.; Park, K.-M.; Kim, H.; Zin, W.-C.; Choi, M.-G.; Kim, K. *Chem. Mater.* **1998**, *10*, 1889−93.
(14) Ardizzoia, G. A.; La Monica, G.; Maspero, A.; Masciocchi, N.; Moret, M. *Eur. J. Inorg. Chem.* **1999**, 1301−7.
(15) Ehlert, M. K.; Rettig, S. J.; Storr, A.; Thompson, R. C.; Trotter, J. *Can. J. Chem.* **1990**, *68*, 1444−9.
(16) Raptis, R. G.; Fackler, J. P., Jr. *Inorg. Chem.* **1990**, *29*, 5003−6.

10.1021/ic062374k CCC: $37.00
Published on Web 03/22/2007

systems,[10,40] acid/base and host/guest chemistry,[34] and as luminescent materials.[23,27,32,34,41]

An area of research activity in our laboratory concerns the chemistry of Cu(I), Ag(I), and Au(I) complexes of fluorinated pyrazolate ligands.[19,27,30,34,38−40,42] Although fluoro substituents usually provide favorable properties such as volatility and thermal and oxidative stability, and coinage metal pyrazolates have been investigated for many years,[43] the coinage metal complexes of *fluorinated pyrazolates* have gained relatively less attention. Our first contribution to this area concerns the synthesis of $\{[3,5\text{-}(CF_3)_2Pz]Cu\}_3$ and $\{[3,5\text{-}(CF_3)_2Pz]Ag\}_3$ ($[3,5\text{-}(CF_3)_2Pz]^-$ = 3,5-bis(trifluoromethyl)pyrazolate, Figure 1).[19] These metal adducts and the related gold analog display fascinating luminescence properties. For example, $\{[3,5\text{-}(CF_3)_2Pz]Cu\}_3$ shows bright luminescence upon exposure to UV radiation. The emission colors of solids and frozen solutions of the trimeric compounds, such as $\{[3,5\text{-}(CF_3)_2Pz]Cu\}_3$, show interesting trends with dramatic sensitivities to temperature, solvent, concentration, and excitation wavelengths.[27,34] These trinuclear coinage metal pyrazolates also exhibit interesting π-acid/base properties, and the acidity and basicity can be controlled by the substituents on the pyrazole ring, as well as by the metal atom.[34] For example, $\{[3,5\text{-}(CH_3)_2Pz]Au\}_3$ is a π-base, whereas the fluorinated analog $\{[3,5\text{-}(CF_3)_2Pz]Au\}_3$ is a π-acid. Toluene and $\{[3,5\text{-}(CF_3)_2Pz]Au\}_3$ form extended columnar structures through face-to-face contacts between the dimer-of-trimer units of the gold pyrazolate and toluene.[34]

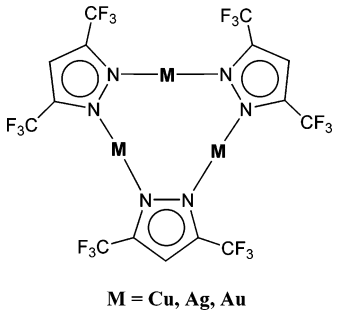

M = Cu, Ag, Au

Figure 1. Coinage metal complexes of 3,5-bis(trifluoromethyl)pyrazolates.

In this paper, we describe the synthesis of a series of silver(I) adducts containing fluorinated pyrazolate ligands and some of their solid-state structures. In particular, we have examined the effect of pyrazolyl ring substituents on the structure because, with Cu(I) and Au(I), bulky groups on pyrazolates lead to tetramers and even hexamers rather than the common trimers.[9,31,44−46] While this work is in progress, the synthesis of $\{[3\text{-}(CF_3),5\text{-}(Bu^t)Pz]Ag\}_3$ and its use as a CVD precursor for the deposition of silver appeared in the literature.[22] The only other report on a fluorinated silver pyrazolate concerns our work on structural, photophysical, and computational studies on $\{[3,5\text{-}(CF_3)_2Pz]Ag\}_3$ and its reactivity with nitrogen-containing heterocycles.[19,34,40,42]

Experimental Section

General Procedures. All manipulations were carried out under an atmosphere of purified nitrogen using standard Schlenk techniques. Solvents were purchased from commercial sources, distilled from conventional drying agents, and degassed by the freeze−pump−thaw method twice prior to use. The glassware was oven dried at 150 °C overnight. NMR spectra were recorded at 25 °C on a JEOL Eclipse 500 spectrometer (^{1}H, 500.16 MHz; ^{19}F, 470.62 MHz). Proton chemical shifts are reported in parts per million versus Me_4Si. ^{19}F NMR chemical shifts were referenced relative to external $CFCl_3$. Infrared spectra were recorded on a JASCO FT-IR 410 spectrometer. Melting points were obtained on a Mel-Temp II apparatus and were not corrected. Elemental analyses were performed using a Perkin-Elmer Model 2400 CHN analyzer. [3-(CF_3)-Pz]H,[47] [3-(CF_3),5-(CH_3)Pz]H,[48] [3-(CF_3),5-(Ph)Pz]H,[49] [3-(C_3F_7),5-

(17) Meyer, F.; Jacobi, A.; Zsolnai, L. *Chem. Ber./Recl.* **1997**, *130*, 1441−7.
(18) Ford, P. C.; Cariati, E.; Bourassa, J. *Chem. Rev.* **1999**, *99*, 3625−47.
(19) Dias, H. V. R.; Polach, S. A.; Wang, Z. *J. Fluorine Chem.* **2000**, *103*, 163−9.
(20) Masciocchi, N.; Cairati, P.; Sironi, A. *Powder Diffr.* **1998**, *13*, 35−40.
(21) Masciocchi, N.; Moret, M.; Cairati, P.; Sironi, A.; Ardizzoia, G. A.; La Monica, G. *J. Am. Chem. Soc.* **1994**, *116*, 7668−76.
(22) Chi, Y.; Lay, E.; Chou, T.-Y.; Song, Y.-H.; Carty, A. J. *Chem. Vap. Deposition* **2005**, *11*, 206−12.
(23) Enomoto, M.; Kishimura, A.; Aida, T. *J. Am. Chem. Soc.* **2001**, *123*, 5608−9.
(24) Burini, A.; Bravi, R.; Fackler, J. P., Jr.; Galassi, R.; Grant, T. A.; Omary, M. A.; Pietroni, B. R.; Staples, R. J. *Inorg. Chem.* **2000**, *39*, 3158−65.
(25) Mohamed, A. A.; Perez, L. M.; Fackler, J. P. *Inorg. Chim. Acta* **2005**, *358*, 1657−62.
(26) Burini, A.; Mohamed, A. A.; Fackler, J. P. *Comments Inorg. Chem.* **2003**, *24*, 253−80.
(27) Dias, H. V. R.; Diyabalanage, H. V. K.; Rawashdeh-Omary, M. A.; Franzman, M. A.; Omary, M. A. *J. Am. Chem. Soc.* **2003**, *125*, 12072−3.
(28) Maspero, A.; Brenna, S.; Galli, S.; Penoni, A. *J. Organomet. Chem.* **2003**, *672*, 123−9.
(29) Yang, G.; Raptis, R. G. *Inorg. Chem.* **2003**, *42*, 261−3.
(30) Omary, M. A.; Rawashdeh-Omary, M. A.; Diyabalanage, H. V. K.; Dias, H. V. R. *Inorg. Chem.* **2003**, *42*, 8612−4.
(31) Fujisawa, K.; Ishikawa, Y.; Miyashita, Y.; Okamoto, K.-I. *Chem. Lett.* **2004**, *33*, 66−7.
(32) Dodge, M. W.; Wacholtz, W. F.; Mague, J. T. *J. Chem. Crystallogr.* **2005**, *35*, 5−12.
(33) Kishimura, A.; Yamashita, T.; Aida, T. *J. Am. Chem. Soc.* **2005**, *127*, 179−83.
(34) Omary, M. A.; Rawashdeh-Omary, M. A.; Gonser, M. W. A.; Elbjeirami, O.; Grimes, T.; Cundari, T. R.; Diyabalanage, H. V. K.; Gamage, C. S. P.; Dias, H. V. R. *Inorg. Chem.* **2005**, *44*, 8200−10.
(35) Torralba, M. C.; Ovejero, P.; Mayoral, M. J.; Cano, M.; Campo, J. A.; Heras, J. V.; Pinilla, E.; Torres, M. R. *Helv. Chim. Acta* **2004**, *87*, 250−63.
(36) Yamada, S.; Ishida, T.; Nogami, T. *Dalton Trans.* **2004**, 898−903.
(37) Mohamed, A. A.; Burini, A.; Fackler, J. P., Jr. *J. Am. Chem. Soc.* **2005**, *127*, 5012−3.
(38) Dias, H. V. R.; Diyabalanage, H. V. K.; Eldabaja, M. G.; Elbjeirami, O.; Rawashdeh-Omary, M. A.; Omary, M. A. *J. Am. Chem. Soc.* **2005**, *127*, 7489−501.
(39) Dias, H. V. R.; Diyabalanage, H. V. K. *Polyhedron* **2006**, *25*, 1655−61.
(40) Grimes, T.; Omary, M. A.; Dias, H. V. R.; Cundari, T. R. *J. Phys Chem. A* **2006**, *110*, 5823−30.
(41) Omary, M. A.; Mohamed, A. A.; Rawashdeh-Omary, M. A.; Fackler, J. P. *Coord. Chem. Rev.* **2005**, *249*, 1372−81.
(42) Dias, H. V. R.; Diyabalanage, H. V. K.; Gamage, C. S. P. *Chem. Commun.* **2005**, 1619−21.
(43) Buchner, E. *Berichte* **1889**, *22*, 842.
(44) Ardizzoia, G. A.; Cenini, S.; La Monica, G.; Masciocchi, N.; Moret, M. *Inorg. Chem.* **1994**, *33*, 1458−63.
(45) Yang, G.; Raptis, R. G. *Inorg. Chim. Acta* **2003**, *352*, 98−104.
(46) Raptis, R. G.; Murray, H. H., III; Fackler, J. P., Jr. *Chem. Commun.* **1987**, 737−9.
(47) Gerus, I. I.; Gorbunova, M. G.; Vdovenko, S. I.; Yagupol'skii, Y. L.; Kukhar, V. P. *Zh. Org. Khim.* **1990**, *26*, 1877−83.
(48) Atwood, J. L.; Dixon, K. R.; Eadie, D. T.; Stobart, S. R.; Zaworotko, M. J. *Inorg. Chem.* **1983**, *22*, 774−9.
(49) Dias, H. V. R.; Goh, T. K. H. H. *Polyhedron* **2004**, *23*, 273−282.

Table 1. ^{1}H NMR and ^{19}F NMR Spectroscopic Data in $CDCl_3$ at Room Temperature

pyrazole	^{1}H	^{19}F	silver pyrazolate	^{1}H	^{19}F
[3-(CF_3)Pz]H	6.63 (s, 1H) 7.67 (s, 1H) 12.34 (br s, 1H)	−61.7 (s)	{[3-(CF_3)Pz]Ag}$_3$	6.68 (br s, 3H) 7.53 (br s, 3H)	−60.2 (s)
[3-(CF_3),5-(CH_3)Pz]H	1.34 (s, 3H) 6.31 (s, 1H) 11.82 (br s, 1H)	−61.9 (s)	{[3-(CF_3),5-(CH_3)Pz]Ag}$_3$	2.26 (s, 9H) 6.39 (s, 3H)	−59.4 (s)
[3-(CF_3),5-(Ph)Pz]H	6.77 (s, 1H) 7.42 (m, 1H) 7.47 (m, 2H) 7.57 (m, 2H) 10.67 (br s, 1H)	−62.2 (s)	{[3-(CF_3),5-(Ph)Pz]Ag}$_3$	6.82 (s, 3H) 7.50 (m, 9H) 7.68 (m, 6H)	−60.2 (s)
[3-(CF_3),5-(Bu^t)Pz]H	1.34 (s, 9H) 6.31 (s, 1H) 10.29 (br s, 1H)	−62.2 (s)	{[3-(CF_3),5-(Bu^t)Pz]Ag}$_3$	1.49 (s, 27H) 6.56 (s, 3H)	−59.5 (s)
[3-(C_3F_7),5-(Bu^t)Pz]H	1.34 (s, 9H) 6.34 (s, 1H) 10.31(br s, 1H)	−80.2 (t, 3F, J = 9.79 Hz) −110.6 (q, 2F, J = 9.79 Hz) −126.9 (s, 2F)	{[3-(C_3F_7),5-(Bu^t)Pz]Ag}$_3$	1.35 (s, 27H) 6.42 (s, 3H)	−79.9 (t, 9F, J = 9.79 Hz) −108.4 (br s, 6F) −126.0 (s, 6F)

(Bu^t)Pz]H,[50] [3-(CF_3),5-(Bu^t)Pz]H,[50] and {[3,5-(CF_3)$_2$Pz]Ag}$_3$[19] were prepared by literature methods. The ^{1}H and ^{19}F NMR data are summarized in Table 1.

{[3-(CF_3)Pz]Ag}$_3$. Ag_2O (0.31 g, 1.34 mmol) and [3-(CF_3)Pz]H (0.37 g, 2.67 mmol) were mixed in toluene (15.0 mL). The resulting mixture was protected from light using aluminum foil and was refluxed overnight. After it was cooled, the solution was filtered through a bed of Celite to remove insoluble material. The filtrate was collected, and the solvent was removed under reduced pressure to yield {[3-(CF_3)Pz]Ag}$_3$ as a white solid. Yield: 88%. mp: 192−195 °C. IR (KBr, cm^{-1}): $\bar{\nu}$ 1724, 1520, 1346, 1245, 1171, 1115, 991, 783. Anal. Calcd for $C_{12}H_6Ag_3N_6F_9$: C, 19.78; H, 0.83; N, 11.53. Found: C, 20.28; H, 0.90; N, 11.55.

{[3-(CF_3),5-(CH_3)Pz]Ag}$_3$. Ag_2O (0.42 g, 1.82 mmol) and [3-(CF_3),5-(CH_3)Pz]H (0.50 g, 3.30 mmol) were mixed in toluene (20.0 mL). The resulting mixture was protected from light using aluminum foil and was refluxed overnight. After it was cooled, the solution was filtered through a bed of Celite. The filtrate was collected, and the solvent was removed under reduced pressure to produce {[3-(CF_3),5-(CH_3)Pz]Ag}$_3$ as a colorless solid. X-ray quality crystals were grown from hexane at 5 °C. Yield: 95%. mp: 270−273 °C (dec). IR (KBr, cm^{-1}): $\bar{\nu}$ 3143, 2927, 2362, 1535, 1485, 1458, 1342, 1242, 1173, 1138, 1001, 791. Anal. Calcd for $C_{15}H_{12}Ag_3N_6F_9$: C, 23.37; H, 1.57; N, 10.9. Found: C, 23.48; H, 1.45; N, 10.92.

{[3-(CF_3),5-(Ph)Pz]Ag}$_3$. Ag_2O (0.14 g, 0.60 mmol) and [3-(CF_3),5-(Ph)Pz]H (0.35 g, 1.19 mmol) were mixed in toluene (20.0 mL). The resulting mixture was protected from light using aluminum foil and was refluxed overnight. After it was cooled, the solution was filtered through a bed of Celite to remove insoluble black material. The filtrate was collected, and the solvent was removed under reduced pressure to give {[3-(CF_3),5-(Ph)Pz]Ag}$_3$ as an off-white solid. The product was recrystallized using toluene/CH_2Cl_2. Yield: 97%. mp: 199−201 °C (dec). IR (KBr, cm^{-1}): $\bar{\nu}$ 3045, 2962, 1604, 1541, 1510, 1461, 1427, 1281, 1250, 1157, 1117, 1011, 910, 804, 762, 690. Anal. Calcd for $C_{30}H_{18}Ag_3N_6F_9$: C, 37.65; H, 1.90; N, 8.78. Found: C, 37.91; H, 1.45; N, 9.17.

{[3-(CF_3),5-(Bu^t)Pz]Ag}$_3$. Ag_2O (0.21 g, 0.91 mmol) and [3-(CF_3),5-(Bu^t)Pz]H (0.32 g, 1.65 mmol) were mixed in toluene (15.0 mL). The resulting mixture was protected from light using aluminum foil and refluxed overnight. After it was cooled, the solution was filtered through a bed of Celite to remove some insoluble black material. The filtrate was collected, and the solvent was removed under reduced pressure to obtain {[3-(CF_3),5-(Bu^t)-Pz]Ag}$_3$ as a yellowish white solid. X-ray quality crystals were grown from dichloromethane/hexane at 5 °C. Yield: 88%. mp: 124−126 °C. IR (KBr, cm^{-1}): $\bar{\nu}$ 3174, 3111, 3055, 2970, 2871, 2362, 1574, 1502, 1483, 1464, 1425, 1392, 1369, 1302, 1257, 1221, 1165, 1136, 1088, 1041, 1011, 982, 806, 746. Anal. Calcd for $C_{24}H_{30}F_9N_3Ag_3$: C, 32.13; H, 3.37; N, 9.37. Found: C, 33.43; H, 3.40; N, 9.37.

{[3-(C_3F_7),5-(Bu^t)Pz]Ag}$_3$. A mixture of Ag_2O (0.21 g, 0.91 mmol) and [3-(C_3F_7),5-(Bu^t)Pz]H (0.38 g, 1.65 mmol) in toluene (15.0 mL) was protected from light using aluminum foil and refluxed overnight. After it was cooled, the solution was filtered through a bed of Celite, and the filtrate was collected. The solvent was removed under reduced pressure to obtain {[3-(C_3F_7),5-(Bu^t)-Pz]Ag}$_3$ as a colorless solid. X-ray quality crystals were grown from hexane at 5 °C. Yield: 92%. mp: 183−185 °C. IR (KBr, cm^{-1}): $\bar{\nu}$ 3186, 3105, 2972, 1653, 1570, 1454, 1417, 1371, 1348, 1298, 1223, 1184, 1119, 1011, 995, 877, 748. Anal. Calcd for $C_{30}H_{30}Ag_3N_6F_{21}$: C, 30.10; H, 2.53; N, 7.02. Found: C, 30.86; H, 2.76; N, 6.78. X-ray quality crystals were grown from toluene at 5 °C, resulting in the formation of a sandwich complex **{[Ag$_3$]′·**[toluene]}$_\infty$ ({[3-(C_3F_7),5-(Bu^t)Pz]Ag}$_3$ = **[Ag$_3$]′**). mp: 174−176 °C. ^{1}H NMR ($CDCl_3$): δ 1.35 (s, 27H, Bu^t), 2.33 (s, 3H, tol-CH_3), 6.42 (s, 3H, Pz-H), 7.17 (m, 5H, tol-H). ^{19}F NMR ($CDCl_3$): δ −79.9 (t, 3F, CF_3, J_{FF} = 9.79 Hz), −108.4 (br s, 2F, CF_2), −126.0 (s, 2F, CF_2). Anal. Calcd for $C_{37}H_{38}N_6F_{21}Ag_3$: C, 34.47; H, 2.97; N, 6.52. Found: C, 34.91; H, 2.66; N, 6.15.

{[Ag$_3$]$_2$·[toluene]}$_\infty$ ({[3,5-(CF_3)$_2$Pz]Ag}$_3$ = [Ag$_3$]). {[3,5-(CF_3)$_2$Pz]Ag}$_3$ (0.50 g, 0.536 mmol) was dissolved in 2.5 mL of toluene and kept at 5 °C to obtain X-ray quality crystals of **{[Ag$_3$]$_2$·**[toluene]}$_\infty$. mp: 220 °C. ^{1}H NMR ($CDCl_3$): δ 2.31 (s, tol-CH_3), 7.03 (s, Pz-H), 7.17 (m, tol-H). ^{19}F NMR ($CDCl_3$): δ −60.9 (s, CF_3). Anal. Calcd for $C_{37}H_{14}N_{12}F_{36}Ag_6$: C, 22.70; H, 0.72; N, 8.59. Found: C, 23.23; H, 0.69; N, 8.12.

X-ray Crystallographic Data. A suitable crystal of the silver complex covered with a layer of hydrocarbon oil was selected, mounted with paratone-N oil in a cryoloop, and immediately placed in the low-temperature nitrogen stream for the low-temperature work or mounted on a glass fiber using five minute epoxy glue for room temperature data collections. The X-ray intensity data of {[3-(CF_3),5-(CH_3)Pz]Ag}$_3$, **{[Ag$_3$]$_2$·**[toluene]}$_\infty$, and **{[Ag$_3$]′·**[toluene]}$_\infty$ were measured at 100(2) K on a Bruker SMART APEX CCD area detector system equipped with a Oxford Cryosystems 700 Series cooler, a graphite monochromator, and a Mo Kα fine-focus sealed tube (λ = 0.710 73 Å). The detector was placed at a

(50) Zelenin, K. N.; Tugusheva, A. R.; Yakimovich, S. I.; Alekseev, V. V.; Zerova, E. V. *Chem. Heterocycl. Compd.* **2002**, *38*, 668−76.

Table 2. X-ray Crystallographic Data for {[3-(CF_3),5-(CH_3)Pz]Ag}$_3$, {[3-(CF_3),5-(Bu^t)Pz]Ag}$_3$, {[3-(C_3F_7),5-(Bu^t)Pz]Ag}$_3$, {**[Ag$_3$]$_2$·**[toluene]}$_\infty$, and {**[Ag$_3$]′·**[toluene]}$_\infty$ (**[Ag$_3$]** = {[3,5-(CF_3)$_2$Pz]Ag}$_3$, **[Ag$_3$]′** = {[3-(C_3F_7),5-(Bu^t)Pz]Ag}$_3$)

	{[3-(CF_3),5-(CH_3)Pz]Ag}$_3$	{[3-(CF_3),5-(Bu^t)Pz]Ag}$_3$	{[3-(C_3F_7),5-(Bu^t)Pz]Ag}$_3$	{**[Ag$_3$]′·**[toluene]}$_\infty$	{**[Ag$_3$]$_2$·**[toluene]}$_\infty$
empirical formula	$C_{15}H_{12}Ag_3F_9N_6$	$C_{24}H_{30}Ag_3F_9N_6$	$C_{30}H_{30}Ag_3F_{21}N_6$	$C_{37}H_{38}Ag_3F_{21}N_6$	$C_{18.50}H_7Ag_3F_{18}N_6$
fw	770.89	897.15	1197.21	1289.34	978.91
temp	100(2) K	293(2) K	293(2) K	100(2) K	100(2) K
wavelength	0.71073 Å	0.71073 Å	0.71073 Å	0.71073 Å	0.71073 Å
cryst syst	triclinic	monoclinic	monoclinic	monoclinic	triclinic
space group	$P\bar{1}$	$P2_1/n$	$P2_1/c$	$P2_1/c$	$P\bar{1}$
unit cell dimensions					
a	8.4759(9) Å	14.452(2) Å	12.2012(14) Å	15.4624(8) Å	13.1022(5) Å
b	11.0492(12) Å	10.0648(17) Å	30.843(4) Å	25.0706(13) Å	22.6659(8) Å
c	12.1947(13) Å	21.350(4) Å	11.477(2) Å	12.3999(6) Å	23.6928(9) Å
α	68.974°	90°	90°	90°	77.841(1)°
β	77.129(1)°	93.223(11)°	103.525(12)°	107.197(1)°	75.896(1)°
γ	83.360(1)°	90°	90°	90°	89.568(1)°
vol	1038.43(19) Å^3	3100.6(9) Å^3	4199.4(10) Å^3	4591.9(4) Å^3	6666.8(4) Å^3
Z	2	4	4	4	10
density (calcd)	2.466 Mg/m^3	1.922 Mg/m^3	1.894 Mg/m^3	1.865 Mg/m^3	2.439 Mg/m^3
R1, wR2 [$I > 2\sigma(I)$]	0.0231, 0.0587	0.0275, 0.0634	0.0590, 0.1541	0.0214, 0.0517	0.0298, 0.0727
R1, wR2 (all data)	0.0250, 0.0600	0.0358, 0.0668	0.0829, 0.1653	0.0248, 0.0537	0.0340, 0.0752

distance of 5.995 cm from the crystal. The data frames were integrated with the Bruker SAINT-Plus software package. Data were corrected for absorption effects using the multiscan technique (SADABS). The X-ray intensity data of {[3-(CF_3),5-(Bu^t)Pz]Ag}$_3$ and {[3-(C_3F_7),5-(Bu^t)Pz]Ag}$_3$ were measured at room temperature on a Siemens P4 diffractometer equipped with graphite-monochromated Mo Kα radiation (λ = 0.710 73 Å). The absorption corrections for these two crystals were based on ψ scan data. The structures were solved and refined using Bruker SHELXTL (version 6.14). A summary of the X-ray data are presented in Table 2. Further details of the data collection and refinement are given in the Supporting Information (CIF file).

{[3-(CF_3),5-(CH_3)Pz]Ag}$_3$ crystallizes in the $P\bar{1}$ space group as a dimer of trimers. The dimer of trimers sits on an inversion center. In each pyrazolyl group, the 3- and 5-positions show either a CF_3/CH_3 or CH_3/CF_3 occupancy pattern (i.e., each site is partially occupied by CF_3 or CH_3), indicating positional disorder. This disorder was resolved satisfactorily, and the site occupancies were refined. All the non-hydrogen atoms were refined anisotropically. The hydrogen atoms were placed at calculated positions and refined using a riding model. The final full-matrix least-squares refinement on F^2 with 388 variables converged at R1 = 2.31% for observed data and wR2 = 6.00% for all data. The goodness-of-fit was 1.042.

{[3-(CF_3),5-(Bu^t)Pz]Ag}$_3$ crystallizes in the $P2_1/n$ space group. {[3-(CF_3),5-(Bu^t)Pz]Ag}$_3$ adopts a bowl shape. Two of the three CF_3 groups show rotational disorder. It was modeled successfully. All the non-hydrogen atoms were refined anisotropically. The hydrogen atoms were placed at calculated positions and refined using a riding model. The final full-matrix least-squares refinement on F^2 with 444 variables converged at R1 = 2.75% for observed data and wR2 = 6.88% for all data. The goodness-of-fit was 1.093.

{[3-(C_3F_7),5-(Bu^t)Pz]Ag}$_3$ crystallizes in the $P2_1/c$ space group. The Ag_3N_6 core is significantly twisted. The fluorine atoms of one of the C_3F_7 groups are disordered, and the disorder in the CF_3 moiety was modeled. All non-hydrogen atoms, except for the atoms of the CF_2CF_3 portion in the disordered C_3F_7 group, were refined anisotropically. The hydrogen atoms were placed at calculated positions and refined using a riding model. The final full-matrix least-squares refinement on F^2 with 519 variables converged at R1 = 5.90% for observed data and wR2 = 16.53% for all data. The goodness-of-fit was 1.038.

{**[Ag$_3$]′·**[toluene]}$_\infty$ (**[Ag$_3$]′** = {[3-(C_3F_7),5-(Bu^t)Pz]Ag}$_3$) crystallizes in the $P2_1/c$ space group. All the non-hydrogen atoms were refined anisotropically. The hydrogen atoms were placed at calculated positions and refined using a riding model. The final full-matrix least-squares refinement on F^2 with 614 variables converged at R1 = 2.14% for observed data and wR2 = 5.37% for all data. The goodness-of-fit was 1.044.

{**[Ag$_3$]$_2$·**[toluene]}$_\infty$ ({**[Ag$_3$]$_2$** = {[3,5-(CF_3)$_2$Pz]Ag}$_3$) crystallizes in the $P\bar{1}$ space group. There are ten {[3,5-(CF_3)$_2$Pz]Ag}$_3$ units and five toluene molecules in the unit cell, and one of the toluene molecules is disordered across a center of symmetry. The bowl-shaped {[3,5-(CF_3)$_2$Pz]Ag}$_3$ units form dimers of trimers. Several CF_3 groups show rotational disorder, which was modeled successfully. The carbon atoms of the disordered toluene molecule were refined isotropically. All other non-hydrogen atoms were refined anisotropically. The hydrogen atoms were placed at calculated positions and refined using a riding model. The final full-matrix least-squares refinement on F^2 with 2130 variables converged at R1 = 2.98% for observed data and wR2 = 7.52% for all data. The goodness-of-fit was 1.020

Results and Discussion

The silver pyrazolates {[3-(CF_3)Pz]Ag}$_3$, {[3-(CF_3),5-(CH_3)Pz]Ag}$_3$, {[3-(CF_3),5-(Ph)Pz]Ag}$_3$, {[3-(CF_3),5-(Bu^t)Pz]Ag}$_3$, and {[3-(C_3F_7),5-(Bu^t)Pz]Ag}$_3$ were prepared by treatment of the corresponding pyrazole with a slight molar excess of silver(I) oxide in toluene (Figure 2).[19,22,39] They were obtained in high yields (>80%). This route provides a convenient and economical method for the synthesis of silver pyrazolates. It also appears to be fairly general because it is possible to use a wide spectrum of pyrazoles such as the electron-rich [3,5-(i-Pr)$_2$Pz]H, weakly coordinating [3,5-(CF_3)$_2$Pz]H, and sterically demanding [3-(C_3F_7),5-(Bu^t)Pz]H successfully in this reaction.[19,22,39]

Silver pyrazolates {[3-(CF_3)Pz]Ag}$_3$, {[3-(CF_3),5-(CH_3)Pz]Ag}$_3$, {[3-(CF_3),5-(Ph)Pz]Ag}$_3$, {[3-(CF_3),5-(Bu^t)Pz]Ag}$_3$, and {[3-(C_3F_7),5-(Bu^t)Pz]Ag}$_3$ are air stable crystalline solids. They are readily soluble in most of the common organic solvents such as hexane, benzene, dichloromethane, acetonitrile, toluene, and tetrahydrofuran. {[3-(CF_3),5-(CH_3)Pz]Ag}$_3$ has the highest melting point (270−273 °C) among the silver pyrazolates illustrated in Figure 2. Others melt near

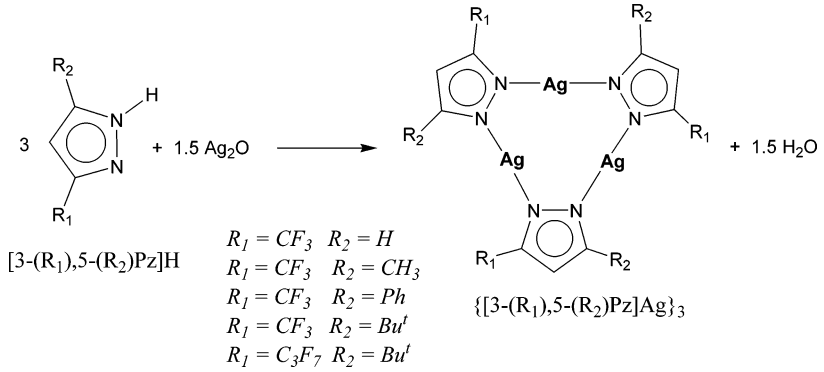

Figure 2. Synthetic route to silver pyrazolates using Ag_2O as the silver source.

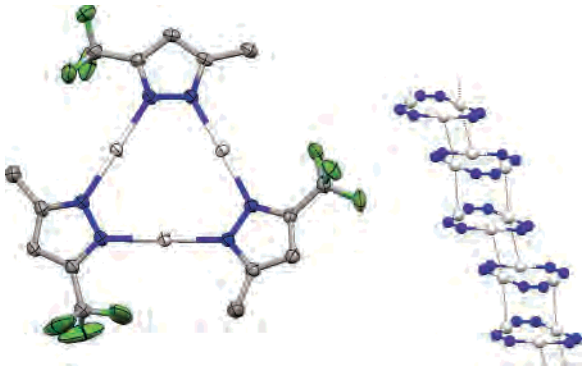

Figure 3. Molecular structure of $\{[3\text{-}(CF_3),5\text{-}(CH_3)Pz]Ag\}_3$ (hydrogen atoms have been omitted for clarity) and the extended chains of $\{[3\text{-}(CF_3),5\text{-}(CH_3)Pz]Ag\}_3$ formed via Ag···Ag contacts (all except nitrogen and silver atoms have been omitted for clarity).

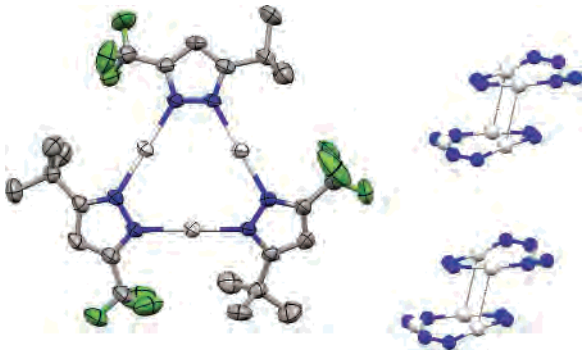

Figure 4. Molecular structure of $\{[3\text{-}(CF_3),5\text{-}(Bu^t)Pz]Ag\}_3$ (hydrogen atoms have been omitted for clarity) and a view showing relative arrangement of the dimers of trimers and the closest Ag···Ag contacts (all except nitrogen and silver atoms have been omitted for clarity).

or below 200 °C. All these silver pyrazolates were characterized using ^1H and ^{19}F NMR spectroscopy (Table 1), FT-IR spectroscopy, and CHN analysis. As expected, the proton NMR spectra of the silver pyrazolates lack the broad peak corresponding to the N−H proton of the free pyrazoles. The ^{19}F NMR spectra of $\{[3\text{-}(CF_3)Pz]Ag\}_3$, $\{[3\text{-}(CF_3),5\text{-}(CH_3)Pz]Ag\}_3$, $\{[3\text{-}(CF_3),5\text{-}(Ph)Pz]Ag\}_3$, and $\{[3\text{-}(CF_3),5\text{-}(Bu^t)Pz]Ag\}_3$ show only one signal each with a chemical shift slightly downfield from that of the respective free pyrazole. The ^1H NMR signal corresponding to the protons at pyrazolyl ring 4-position also shows a small downfield shift.

Compounds $\{[3\text{-}(CF_3),5\text{-}(CH_3)Pz]Ag\}_3$, $\{[3\text{-}(CF_3),5\text{-}(Bu^t)Pz]Ag\}_3$, and $\{[3\text{-}(C_3F_7),5\text{-}(Bu^t)Pz]Ag\}_3$, as well as the π-acid/base adducts $\{\mathbf{[Ag_3]_2}\cdot[\text{toluene}]\}_\infty$ and $\{\mathbf{[Ag_3]'}\cdot$

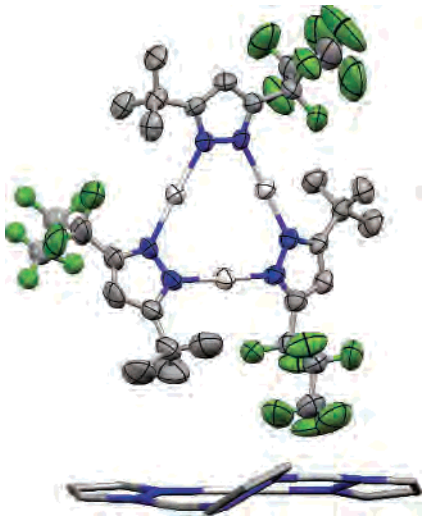

Figure 5. Molecular structure of $\{[3\text{-}(C_3F_7),5\text{-}(Bu^t)Pz]Ag\}_3$ (hydrogen atoms have been omitted for clarity) and a side view showing the twisted Ag_3N_6 core (pyrazolyl ring substituents have been omitted for clarity).

$[\text{toluene}]\}_\infty$ (formed during the isolation of $\{[3\text{-}(C_3F_7),5\text{-}(Bu^t)Pz]Ag\}_3$ and $\{[3,5\text{-}(CF_3)_2Pz]Ag\}_3$ from toluene) were characterized using X-ray crystallography. Despite several attempts, we could not obtain crystals of $\{[3\text{-}(CF_3)Pz]Ag\}_3$ and $\{[3\text{-}(CF_3),5\text{-}(Ph)Pz]Ag\}_3$ suitable for X-ray diffraction studies.

X-ray data of $\{[3\text{-}(CF_3),5\text{-}(CH_3)Pz]Ag\}_3$ show that it adopts a trinuclear structure (Figure 3) with an essentially planar nine-membered Ag_3N_6 metallacycle. Neighboring pairs of these trinuclear units are linked by two equal and relatively short Ag···Ag contacts (3.3553(4) Å) across a crystallographic inversion center. The dimer of trimers interacts further with their neighbors via additional Ag···Ag links (3.4263(4) Å), forming extended stepladder-shaped columns (Figure 3). These Ag···Ag distances are less than the sum of the van der Waals radii of two silver atoms (3.44 Å)[51] but longer than the Ag−Ag distance in the open-shell metallic silver (2.889 Å).[10,51]

$\{[3\text{-}(CF_3),5\text{-}(Bu^t)Pz]Ag\}_3$ also features a trinuclear structure (Figure 4) but has a slightly concave shape. These

(51) (a) For the most widely used, but probably some what underestimated, van der Waals radii, see: Bondi, A. *J. Phys. Chem.* **1964**, *68*, 441−51. (b) For other suggested values, see: Batsanov, S. S. *Inorg. Mater.* **2001**, *37*, 871−85 and references therein.

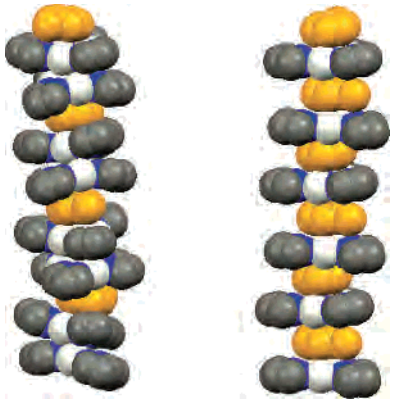

Figure 6. Sandwich structures of {**[Ag$_3$]$_2$**·[toluene]}$_\infty$ (left) and {**[Ag$_3$]′**·[toluene]}$_\infty$ (right): **[Ag$_3$]** = {[3,5-(CF$_3$)$_2$Pz]Ag}$_3$ and **[Ag$_3$]′** = {[3-(C$_3$F$_7$),5-(Bu^t)Pz]Ag}$_3$. Toluene molecules are depicted in yellow. Pyrazolyl ring substituents and hydrogen atoms have been omitted for clarity.

trimers crystallize in pairs, essentially forming dimers of trimers. The six silver atom core of the two trimer units adopts a chair conformation. Even the closest intertrimer Ag···Ag separation (3.4804(7) Å) in {[3-(CF$_3$),5-(Bu^t)Pz]-Ag}$_3$ (see Figure 4) is not as short as the intertrimer Ag···Ag contacts of {[3-(CF$_3$),5-(CH$_3$)Pz]Ag}$_3$. This may be a result of the steric repulsions between the pyrazolyl ring substituents on the adjacent trimers, which prevent the formation of shorter Ag···Ag links. The concave shape of {[3-(CF$_3$),5-(Bu^t)Pz]Ag}$_3$ also appears to be primarily a result of the *inter*trimer steric interactions between the pyrazolyl ring substituents. These repulsions push the pyrazolyl rings away from the mid plane of the dimer of trimers leading to the bowl-shaped conformation. These steric interactions also cause the N−Ag−N angle to deviate significantly from the ideal 180°. For example, the N−Ag−N bond angles of this adduct range from 166.94(16) to 172.99(15)°. In {[3-(CF$_3$),5-(Bu^t)Pz]Ag}$_3$, the neighboring dimer-of-trimer units reside too far apart (e.g., closest Ag···Ag separation = 6.270 Å) to form extended chain structures via Ag···Ag contacts.

Interestingly, despite the presence of two large substituents on the pyrazolyl ring, [3-(C$_3$F$_7$),5-(Bu^t)Pz]Ag also trimerizes and forms the typical trinuclear unit (Figure 5). These trinuclear units pack in a staggered fashion (i.e., with a lateral slippage), forming zigzag chains that do not feature any intertrimer Ag···Ag contacts (the closest separation is at 5.376 Å). The nine-membered Ag$_3$N$_6$ metallacycle in {[3-(C$_3$F$_7$),5-(Bu^t)Pz]Ag}$_3$ shows a significant deviation from planarity. Although it is tempting to attribute this solely to the intratrimer steric effects of having C$_3$F$_7$ and *t*-butyl substituents on the adjacent pyrazolyl ligands, the relatively planar Ag$_3$N$_6$ rings in the {[3-(C$_3$F$_7$),5-(Bu^t)Pz]Ag}$_3$·toluene adduct (see below) points to an alternative possibility. It appears that this ring twisting is caused primarily by the intertrimer steric interactions. The C$_3$F$_7$ groups of the {[3-(C$_3$F$_7$),5-(Bu^t)Pz]Ag}$_3$ adduct point above and below the Ag$_3$N$_6$ plane to avoid *t*-butyl substituents on the adjacent pyrazolyl rings. However, this arrangement of the substituents leads to adverse steric interactions with the neighboring trimers causing large ring distortions in the {[3-(C$_3$F$_7$),5-(Bu^t)Pz]Ag}$_3$ units. There are also close intertrimer Ag···F (3.096 Å) contacts.[52,53] These distances are within the sum of the van der Waals radii of Ag and F (3.19 Å).[54] There are also somewhat close (2.89 Å; cf. van der Waals contact of Ag and H, 2.92 Å) intertrimer Ag···H contacts between silver atoms and one of the hydrogens of the *t*-butyl group. However, these Ag···H and Ag···F contacts may not be that significant considering that they are not notably shorter than the van der Waals contact distance and are probably a result of crystal packing.

Overall, X-ray crystallographic data of molecules like {[3-(CF$_3$),5-(Bu^t)Pz]Ag}$_3$ and {[3-(C$_3$F$_7$),5-(Bu^t)Pz]Ag}$_3$ show that silver pyrazolates can accommodate large substituents on the pyrazolyl ring 3- and 5-positions while maintaining the trinuclear structures with Ag$_3$N$_6$ cores. Tetramers like {[3,5-(Bu^t)$_2$Pz]Ag}$_4$, reported recently by Raptis et al., are very rare among silver pyrazolates.[55] This is probably a direct result of the size of the coinage metal ion. Silver is the largest member of the coinage metal family. For comparison, the covalent radii of two-coordinate Cu(I), Ag(I), and Au(I) are 1.11, 1.33, and 1.25 Å, respectively.[34,56] With copper and gold pyrazolates, bulky substituents at the 3- and 5-position of the pyrazolyl moiety often lead to different aggregates such as tetramers and even hexamers.[9,31,44−46]

Selected bond distances and angles of trimeric silver(I) pyrazolates are listed in Table 3. Data show that the Ag−N bond distances of {[(3-(CF$_3$),5-(CH$_3$)Pz]Ag}$_3$, {[3-(CF$_3$),5-(Bu^t)Pz]Ag}$_3$, and {[3-(C$_3$F$_7$),5-(Bu^t)Pz]Ag}$_3$ are very similar. Even silver pyrazolates bearing much more weakly coordinating pyrazolates or electron rich pyrazolates have similar Ag−N bond lengths. For example, the ranges of the Ag−N bond distances of {[3,5-(CF$_3$)$_2$Pz]Ag}$_3$[19] and {[3,5-(*i*-Pr)$_2$Pz]Ag}$_3$[39] are 2.081(3)−2.096(3) and 2.048(3)−2.088-(3) Å, respectively. Thus, steric-electronic effects of pyrazolyl ring substituents have essentially no effect on the Ag−N bond lengths of these adducts. The N−Ag−N angles, however, display significant variations. For example, each silver site in {[3-(CF$_3$),5-(CH$_3$)Pz]Ag}$_3$ shows linear coordination to pyrazolyl nitrogens. The N−Ag−N angles range from 177.78(10)−178.62(10)°. This molecule contains relatively smaller substituents on the pyrazolyl rings. The N−Ag−N bond angle range is somewhat wider and the deviation from ideal 180° is greater in the adducts {[3-(CF$_3$),5-(Bu^t)Pz]Ag}$_3$ and {[3-(C$_3$F$_7$),5-(Bu^t)Pz]Ag}$_3$ bearing bulky pyrazolyl ring substituents. As described earlier, the distortions in these two latter molecules are primarily a result of the intertrimer steric repulsions. A twisting of the Ag$_3$N$_6$ core (Figure 5) is an option to alleviate steric repulsions when the molecules are not constrained by the intertrimer metallophilic contacts. However, when the metal atoms of the adjacent trimers are close, as in {[3-(CF$_3$),5-(Bu^t)Pz]Ag}$_3$

(52) Plenio, H. *Chem. Rev.* **1997**, *97*, 3363−84.
(53) Plenio, H. *Chem. Bio. Chem.* **2004**, *5*, 650−5.
(54) Winter, M. Webelements Periodic Table, professional edition, 2006, http://www.webelements.com/.
(55) Guang, Y.; Raptis, R. G. *Inorg. Chim. Acta* [Online early access] DOI: 10.1016/j.ica.2006.10.032. Published Online: Nov 9, 2006.
(56) Bayler, A.; Schier, A.; Bowmaker, G. A.; Schmidbaur, H. *J. Am. Chem. Soc.* **1996**, *118*, 7006−7.

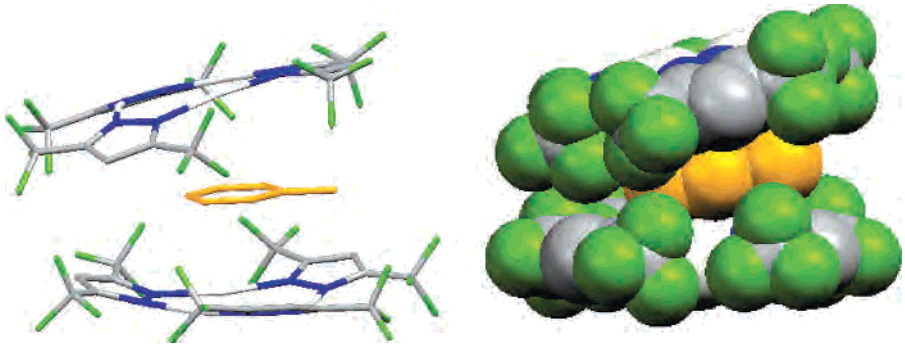

Figure 7. View showing the toluene molecule sandwiched between the two $\{[3,5\text{-}(CF_3)_2Pz]Ag\}_3$ trimers as in a clam shell.

Table 3. Bond Distances (Å) and Angles (deg) for $\{[3\text{-}(CF_3),5\text{-}(CH_3)Pz]Ag\}_3$, $\{[3\text{-}(CF_3),5\text{-}(Bu^t)Pz]Ag\}_3$, $\{[3\text{-}(C_3F_7),5\text{-}(Bu^t)Pz]Ag\}_3$, $\{[3,5\text{-}(CF_3)_2Pz]Ag\}_3$, $\{[3,5\text{-}(i\text{-}Pr)_2Pz]Ag\}_3$, $\{\mathbf{[Ag_3]_2}\cdot[\text{toluene}]\}_\infty$, and $\{\mathbf{[Ag_3]'}\cdot[\text{toluene}]\}_\infty$ (**[Ag$_3$]** = $\{[3,5\text{-}(CF_3)_2Pz]Ag\}_3$, **[Ag$_3$]′** = $\{[3\text{-}(C_3F_7),5\text{-}(Bu^t)Pz]Ag\}_3$)

	$\{[3\text{-}(CF_3),5\text{-}(CH_3)Pz]Ag\}_3$	$\{[3\text{-}(CF_3),5\text{-}(Bu^t)Pz]Ag\}_3$	$\{[3\text{-}(C_3F_7),5\text{-}(Bu^t)Pz]Ag\}_3$	$\{[3,5\text{-}(CF_3)_2Pz]Ag\}_3$
Ag−N (range)	2.076(3)−2.084(3)	2.086(3)−2.093(4)	2.084(8)−2.095(8)	2.081(3)−2.096(3)
Ag···Ag (intra, range)	3.392−3.493	3.413−3.489	3.394−3.448	3.440−3.541
Ag···Ag(inter, shortest)	3.3553(4)	3.4804(7)	5.376	3.2037(4)
N−Ag−N (range)	177.78(10)−178.62(10)	166.94(16)−172.99(15)	174.1(4)−179.3(3)	172.01(12)−177.69(13)

	$\{[3,5\text{-}(i\text{-}Pr)_2Pz]Ag\}_3$	$\{\mathbf{[Ag_3]_2}\cdot[\text{toluene}]\}_\infty$	$\{\mathbf{[Ag_3]'}\cdot[\text{toluene}]\}_\infty$
Ag−N (range)	2.048(3)−2.088(3)	2.075(3)−2.108(3)	2.098(14)−2.110(14)
Ag···Ag (intra, range)	3.324−3.489	3.440−3.449	3.394−3.409
Ag···Ag (inter, shortest)	2.9870(4)	3.0911(4)	
N−Ag−N (range)	170.21(13)−177.68(13)	171.42(13)−179.26(14)	175.17(6)−177.27(6)

(or show metallophilic bonding as in dimers of $\{[3,5\text{-}(i\text{-}Pr)_2,4\text{-}(Br)Pz]Ag\}_3$),[39] trimers seem to adopt a bowl shape to relieve the steric repulsions while preserving the budding (or existing) Ag···Ag linkages.

Trinuclear complexes of monovalent coinage metal ions have very interesting π- acid/base properties.[41,57] However, this property is barely explored in the coinage metal pyrazolate family.[34] Computational studies show that compounds of the type $\{[3,5\text{-}(CF_3)_2Pz]M\}_3$ (M = Cu, Ag, Au) are π-acids with the silver(I) analog having the highest acidity.[34] We have been able to isolate two interesting π-acid/base complexes by exploiting the acidity of $\{[3,5\text{-}(CF_3)_2Pz]Ag\}_3$ and $\{[3\text{-}(C_3F_7),5\text{-}(Bu^t)Pz]Ag\}_3$ and the π-basicity of toluene. The X-ray crystallographic analysis of the crystals of $\{[3,5\text{-}(CF_3)_2Pz]Ag\}_3$ obtained from toluene reveals an interesting supramolecular sandwich structure with the composition $\{\mathbf{[Ag_3]_2}\cdot[\text{toluene}]\}_\infty$ (Figure 6, $\{[3,5\text{-}(CF_3)_2Pz]Ag\}_3$ = **[Ag$_3$]**). $\{[3,5\text{-}(CF_3)_2Pz]Ag\}_3$ units exist as dimers of trimers, **[Ag$_3$]$_2$**. It is possible to identify three types of **[Ag$_3$]$_2$** moieties in these columnar stacks, and they show different types of face-to-face intertrimer contacts (see Supporting information for relevant figures). The six silver atom core of one of these **[Ag$_3$]$_2$** units adopts a distorted trigonal prismatic conformation (with Ag···Ag contacts of 3.252, 3.281, and 3.327 Å), while the other two show two different distorted octahedral arrangements (with closest Ag···Ag separations of 3.091 Å in one, and 3.474 Å in the other). Such structural variations are not surprising because Ag···Ag contacts between the closed-shell d^{10} centers are relatively weak, and the interaction potential is shallow for a considerable Ag···Ag distance range.[40,58] Toluene in $\{\mathbf{[Ag_3]_2}\cdot[\text{toluene}]\}_\infty$ serves as the bridge between dimers of trimers forming extended stacks. Interestingly, the trinuclear $\{[3,5\text{-}(CF_3)_2Pz]Ag\}_3$ units curve toward toluene forming a partially closed "clam shell" shape (Figure 7). In contrast, the parent $\{[3,5\text{-}(CF_3)_2Pz]Ag\}_3$ has a significantly more planar structure.[34] The **[Ag$_3$]** and toluene centroids of $\{\mathbf{[Ag_3]_2}\cdot[\text{toluene}]\}_\infty$ are separated by a distance that ranges from 3.18 to 3.29 Å. The closest Ag···C(toluene) distance is 3.163 Å. These separations are well within the sum of van der Waals radii of Ag and C (3.42 Å),[54] pointing to the presence of relatively tight π-acid/base contacts. The closely related gold complex $\{\mathbf{[Au_3]_2}\cdot[\text{toluene}]\}_\infty$ is known.[34] In this adduct, the **[Au$_3$]** and toluene centroids are separated by 3.43 and 3.86 Å. The closest Au···C(toluene) distance is 3.288 Å. Interestingly, despite the presence of a much smaller metal ion in $\{\mathbf{[Au_3]_2}\cdot[\text{toluene}]\}_\infty$, the **[Au$_3$]** and toluene contacts are significantly longer than the corresponding distances of the $\{\mathbf{[Ag_3]_2}\cdot[\text{toluene}]\}_\infty$. Thus, these data indicate the presence of a much stronger contact between **[Ag$_3$]** and toluene.

The $\{[3\text{-}(C_3F_7),5\text{-}(Bu^t)Pz]Ag\}_3$ forms extended stacks of the type $\{\mathbf{[Ag_3]'}\cdot[\text{toluene}]\}_\infty$ (Figure 6, $\{[3\text{-}(C_3F_7),5\text{-}(Bu^t)Pz]Ag\}_3$ = **[Ag$_3$]′**), which is the most common stacking pattern for trinuclear complexes involving d^{10} metal ions.[59−63]

(57) Olmstead, M. M.; Jiang, F.; Attar, S.; Balch, A. L. *J. Am. Chem. Soc.* **2001**, *123*, 3260−7.

(58) Pyykko, P.; Runeberg, N.; Mendizabal, F. *Chem.—Eur. J.* **1997**, *3*, 1451−7.

(59) Haneline, M. R.; King, J. B.; Gabbai, F. P. *Dalton Trans.* **2003**, 2686−90.

(60) Tsunoda, M.; Gabbaie, F. P. *J. Am. Chem. Soc.* **2000**, *122*, 8335−6.

(61) Burini, A.; Fackler, J. P., Jr.; Galassi, R.; Grant, T. A.; Omary, M. A.; Rawashdeh-Omary, M. A.; Pietroni, B. R.; Staples, R. J. *J. Am. Chem. Soc.* **2000**, *122*, 11264−5.

(62) Rawashdeh-Omary, M. A.; Omary, M. A.; Fackler, J. P., Jr.; Galassi, R.; Pietroni, B. R.; Burini, A. *J. Am. Chem. Soc.* **2001**, *123*, 9689−91.

Table 4. Closest Intertrimer Ag···Ag Distances (Å) for Selected Trinuclear Silver(I) Pyrazolates

compound	closest intertrimer Ag···Ag separation	ref
$\{[3,5\text{-}(Ph)_2Pz]Ag\}_3$ (from CH_2Cl_2)	2.971(1)	25
$\{[3,5\text{-}(i\text{-}Pr)_2Pz]Ag\}_3$	2.9870(4)	39
$\{[3,5\text{-}(i\text{-}PrSCH_2)_2Pz]Ag\}_3$	3.041(1)	17
$\{[3,5\text{-}(i\text{-}Pr)_2,4\text{-}(Br)Pz]Ag\}_3$	3.044(5)	39
$\{[Pz(IN)]Ag\}_3$	3.179(8)	36
$\{[3,5\text{-}(CF_3)_2Pz]Ag\}_3$ (from CH_2Cl_2)	3.2037(4)	34
$\{[2\text{-}(3(5)\text{-}Pz)Py]Ag\}_3$	3.227(2)	10
$\{[3,5\text{-}(CH_3)_2Pz]Ag\}_3$	3.230(13)	20
$\{[3,5\text{-}(CF_3)_2Pz]Ag\}_3$ (from hexane)	3.307(13)	19
$\{[3\text{-}(CF_3),5\text{-}(CH_3)Pz]Ag\}_3$	3.3553(4)	this work
$\{[Pz]Ag\}_3$	3.431(4)	21
sum of Ag−Ag van der Waals radii	3.44	51, 54
$\{[3\text{-}(CF_3),5\text{-}(Bu^t)Pz]Ag\}_3$	3.4804(7)	this work
$\{[3\text{-}(C_3F_7),5\text{-}(Bu^t)Pz]Ag\}_3$	(5.376)	this work

In $\{\mathbf{[Ag_3]'}\cdot[\text{toluene}]\}_\infty$, the **[Ag$_3$]′** and toluene centroids are separated by 3.11 and 3.16 Å. The closest Ag···C(toluene) distance is 3.143 Å. These distances are remarkably close despite the large size of the pyrazolyl ring substituents. It is also interesting to note that the $\{\mathbf{[Ag_3]'}\cdot[\text{toluene}]\}_\infty$ features a significantly more-planer less-twisted Ag_3N_6 metallacycle compared to that seen in the toluene-free **[Ag$_3$]′**. For example, the Ag−N−N−Ag torsion angles of $\{\mathbf{[Ag_3]'}\cdot[\text{toluene}]\}_\infty$ are −2.85, −2.64, and 5.39°, while the corresponding angles of the toluene-free **[Ag$_3$]′** are −1.96, −9.90, and 32.17°. It could be a result of the reduced *inter*trimer steric interactions in $\{\mathbf{[Ag_3]'}\cdot[\text{toluene}]\}_\infty$. Compared to the parent **[Ag$_3$]′**, the $\{[3\text{-}(C_3F_7),5\text{-}(Bu^t)Pz]Ag\}_3$ units of the $\{\mathbf{[Ag_3]'}\cdot[\text{toluene}]\}_\infty$ adduct lie relatively far apart. This leaves more space above and below the $\{[3\text{-}(C_3F_7),5\text{-}(Bu^t)Pz]Ag\}_3$ plane for the C_3F_7 and Bu^t substituents to occupy without interfering with the space demands of the adjacent trimers.

The π-acidic, trinuclear Hg(II) adduct $[o\text{-}C_6F_4Hg]_3$ also forms sandwich complexes with toluene leading to $\{[o\text{-}C_6F_4Hg]_3\cdot[\text{toluene}]\}_\infty$ stacks analogous to those of $\{\mathbf{[Ag_3]'}\cdot[\text{toluene}]\}_\infty$.[59] In $\{[o\text{-}C_6F_4Hg]_3\cdot[\text{toluene}]\}_\infty$, the $[o\text{-}C_6F_4Hg]_3$ and toluene centroids are separated by 3.63 and 3.81 Å. The closest Hg···C(toluene) distance is 3.189 Å. Thus, on the basis of the X-ray data, with consideration of the relatively smaller van der Waals radius of Hg,[54] $\{\mathbf{[Ag_3]'}\cdot[\text{toluene}]\}_\infty$ appears to have somewhat tighter metal···C(toluene) contacts than those of the $\{[o\text{-}C_6F_4Hg]\cdot[\text{toluene}]\}_\infty$.

Tables 3 and 4 show intratrimer and intertrimer $Ag^I\cdots Ag^I$ separations observed for the trinuclear species herein and for few other silver pyrazolates in the literature.[10,17,19−21,25,34,36,39] The silver atoms of these trinuclear species are held in close proximity by the bridging pyrazolate ligands. Thus, the *intra*trimer Ag···Ag distances are primarily controlled by the pyrazolate bridges and have limited freedom for variations. On the other hand, close *inter*trimer Ag···Ag separations, unassisted by bridging ligands or electrostatics, as seen with $\{[3\text{-}(CF_3),5\text{-}(CH_3)Pz]Ag\}_3$ and $\{\mathbf{[Ag_3]_2}\cdot[\text{toluene}]\}_\infty$ are noteworthy, represent genuine examples of argentophilic bonding,[10,64−69] and fall into the general category of *metallophilic bonding*.[69,70] Such metallophilic contacts give rise to the interesting supramolecular structures and specific photophysical properties of coinage metal pyrazolates.[29,34] The Ag···Ag linkages are also important for the catalytic activity of certain silver adducts.[71] As seen from the data presented in Table 4, dimers of $\{[3,5\text{-}(Ph)_2Pz]Ag\}_3$ (obtained from CH_2Cl_2) have the shortest intertrimer Ag···Ag contact among the silver(I) pyrazolates. The corresponding Ag···Ag separation in $\{[3\text{-}(CF_3),5\text{-}(CH_3)Pz]Ag\}_3$ falls at the higher end of the envelope. The intertrimer Ag···Ag separation in the related adduct $\{[3\text{-}(CF_3),5\text{-}(Bu^t)Pz]Ag\}_3$ is slightly longer than the sum of the van der Waals radii of two silver atoms. However, the existence of an attractive force, albeit small, between the silver centers in this molecule cannot be totally ruled out. In fact, computational studies indicate that the metallophilic attractions between coinage metal atoms do not end abruptly at the van der Waals contact limit.[58,70,72,73] For example, unassisted cuprophiclic interactions could exist when the Cu···Cu distances are even at 4.5 Å (cf. van der Waals separation of Cu−Cu = 2.80 Å).[73,74]

Overall, we describe the synthesis of $\{[3\text{-}(CF_3)Pz]Ag\}_3$, $\{[3\text{-}(CF_3),5\text{-}(CH_3)Pz]Ag\}_3$, $\{[3\text{-}(CF_3),5\text{-}(Ph)Pz]Ag\}_3$, $\{[3\text{-}(CF_3),5\text{-}(Bu^t)Pz]Ag\}_3$, and $\{[3\text{-}(C_3F_7),5\text{-}(Bu^t)Pz]Ag\}_3$, as well as two π-acid/base adducts involving silver pyrazolates and toluene. These compounds represent rare silver(I) complexes featuring fluorinated pyrazolates. The structurally characterized adducts show trinuclear structures. Some of these trimers aggregate via intertrimer Ag···Ag contacts leading to dimers of trimers or chains of trimers. The steric bulk of the substituents affects the tendency and nature of aggregation. It also affects the N−Ag−N angles and the orientation of pyrazolyl moieties relative to the Ag_3 plane. Larger substituents on the pyrazolyl ring 3- and 5-positions lead to significant distortions in the planar Ag_3N_6 core. The Ag−N distances are relatively insensitive to the type of pyrazolyl ring substituents. The isolation of sandwich molecules with tight face-to-face contacts between toluene and trinuclear silver adducts points to the high π-acidic nature of $\{[3,5\text{-}(CF_3)_2Pz]Ag\}_3$ and $\{[3\text{-}(C_3F_7),5\text{-}(Bu^t)Pz]Ag\}_3$. We are currently exploring the chemistry and photophysical properties of these silver adducts.

(63) Taylor, T. J.; Burress, C. N.; Pandey, L.; Gabbai, F. P. *Dalton Trans.* **2006**, 4654−4656.
(64) Wang, Q.-M.; Mak, T. C. W. *J. Am. Chem. Soc.* **2001**, *123*, 7594−600.
(65) Rawashdeh-Omary, M. A.; Omary, M. A.; Patterson, H. H. *J. Am. Chem. Soc.* **2000**, *122*, 10371−80.
(66) Che, C.-M.; Tse, M.-C.; Chan, M. C. W.; Cheung, K.-K.; Phillips, D. L.; Leung, K.-H. *J. Am. Chem. Soc.* **2000**, *122*, 2464−68.
(67) Kim, S. A.; Kim, Y. J.; Park, K.-M.; Choi, S. N.; Jung, O.-S. *Bull. Korean Chem. Soc.* **2005**, *26*, 181−3.
(68) Jansen, M. *Angew. Chem., Int. Ed. Engl.* **1987**, *99*, 1136−49.
(69) Tong, M.-L.; Chen, X.-M.; Ye, B.-H.; Ji, L.-N. *Angew. Chem., Int. Ed.* **1999**, *38*, 2237−40.
(70) Pyykko, P. *Chem. Rev.* **1997**, *97*, 597−636.
(71) Cui, Y.; He, C. *J. Am. Chem. Soc.* **2003**, *125*, 16202−3.
(72) Carvajal, M. A.; Alvarez, S.; Novoa Juan, J. *Chem.—Eur. J.* **2004**, *10*, 2117−32.
(73) Hermann, H. L.; Boche, G.; Schwerdtfeger, P. *Chem.—Eur. J.* **2001**, *7*, 5333−42.
(74) Poblet, J.-M.; Benard, M. *Chem. Commun.* **1998**, 1179−80.

Acknowledgment. Support by the AFPSR through the SPRING program in Texas and the Robert A. Welch Foundation (Y-1289) is gratefully acknowledged. We would also like to acknowledge the contributions of Daniel Been and Christopher Lam to silver pyrazolate work. They were supported by the Welch Summer Scholar Program.

Supporting Information Available: X-ray crystallographic data (CIF), ORTEP diagrams, and additional figures for the structurally characterized compounds presented in this manuscript. This material is available free of charge via the Internet at http://pubs.acs.org.

IC062374K